Self-Assembly of Porphyrin Arrays by Hydrogen Bonding in the Solid State: An Orthogonal Porphyrin – Bisresorcinol System

Kenji Kobayashi, Masayuki Koyanagi, Ken Endo, Hideki Masuda, and Yasuhiro Aoyama*

Abstract: The crystal structures of two adducts ($\mathbf{1}\cdot 2H_2O\cdot 2$IBB and $\mathbf{1}\cdot 4$THF; IBB = isobutyl benzoate) of an orthogonal porphyrin – bisresorcinol derivative, the Zn^{II} complex of 5,15-bis(3,5-dihydroxy-1-phenyl)octaethylporphyrin (**1**), are described. Both adducts contain an extensive hydrogen-bonding network, which forces the porphyrin rings into a columnar alignment. The resulting sheets are layered to give either a staggered arrangement (in adduct $\mathbf{1}\cdot 2H_2O\cdot 2$IBB) or herringbone-type edge-to-face contacts (in adduct $\mathbf{1}\cdot 4$THF) of the porphyrin moieties in neighboring sheets. In the large cavities left, guest molecules are incorporated by hydrogen bonding (resorcinol $\cdots$ OH_2 $\cdots$ IBB) in adduct $\mathbf{1}\cdot 2H_2O\cdot 2$IBB, or by a combination of hydrogen bonding (resorcinol $\cdots$ THF) and metal coordination (Zn^{II} $\cdots$ THF) in adduct $\mathbf{1}\cdot 4$THF. The use of the large porphyrin spacer in the orthogonality strategy is discussed in the light of the known crystal structures of related anthracene – bisresorcinol derivatives.

Keywords: crystal engineering · hydrogen-bonded networks · microporosity · porphyrinoids · zeolite analogues

Introduction

Self-assembly[1] of porphyrin derivatives has attracted much recent attention in view of their photoelectronic properties,[2] which may be applicable in molecular devices.[3] The primary electron-transfer step in bacterial photosynthetic reaction center complexes occurs between porphyrinoid species over a distance of ≈17 Å.[4] The light-harvesting system, on the other hand, involves ≈300 chlorophyll molecules, which are spatially and orientationally controlled.[5] Much effort has been devoted to the preparation of finite arrays of porphyrin in solution by linking two or more porphyrin moieties covalently[3c-e,6] or noncovalently.[7] Infinite arrays of porphyrin may be constructed in the solid state by the manipulation of intermolecular interactions.[8]

The crystal structures of porphyrins are governed by strong $\pi-\pi$ stacking interactions.[3a,9,10] Because of their clathrate properties, simple tetraarylporphyrins are referred to as porphyrin sponges.[11] Attempts have been made to achieve an in-plane alignment of porphyrin by formation of a hydrogen-bonded[12] or metal-coordination[13] network. Actually, the crystal structures of Zn^{II} complexes of tetra(4-hydroxy-1-phenyl)porphyrin are highly dependent on the guest molecules incorporated in the crystal lattices.[12]

We have recently introduced the orthogonality strategy and reported the crystal structures of the anthracene – bisresorcinol derivative **2**.[14] An extensive hydrogen-bonded network involving the resorcinol moieties forces the orthogonal anthracene rings to form columns together with large cavities. The latter not only incorporate a variety of guest molecules but also promote intracavity reactions in a catalytic manner.[15] The inter-ring distances of the anthracene moieties are also controllable.[16, 17]

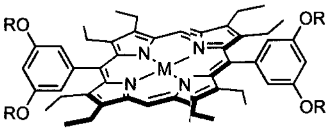

1 : R = H, M = Zn(II)
2 : R = H, M = 2H
3 : R = CH$_3$, M = 2H

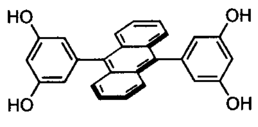

2

The present work is concerned with an analogous metalloporphyrin derivative **1**. The metalloporphyrins are remarkable not only photoelectronically but also as catalysts. The

---

[*] Prof. Dr. Y. Aoyama, M. Koyanagi, Dr. K. Endo
Institute for Fundamental Research of Organic Chemistry, Kyushu University, Hakozaki, Higashi-ku, Fukuoka 812 – 81 (Japan)
CREST, Japan Science and Technology Corporation (JST)
Fax: (+ 92) 642-2719
E-mail: aoyamay@ms.ifoc.kyushu-u.ac.jp
Dr. K. Kobayashi
Department of Chemistry, University of Tsukuba
Tsukuba, Ibaraki 305 (Japan)
Prof. Dr. H. Masuda
Department of Applied Chemistry, Nagoya Institute of Technology
Gokiso-cho, Showa-ku, Nagoya 466 (Japan)
CREST, Japan Science and Technology Corporation (JST)

expected hydrogen-bonded network, if it works, would result in a vertical alignment of the porphyrin rings and the formation of large cavities with porphyrin rings as their roofs and floors. We report here that the hydrogen-bonded network and the supramolecular cavities are well conserved for the porphyrin system too and that the actual modes of guest binding and packing of molecular sheets are guest-dependent.

Results and Discussion

Host – guest adducts: Slow diffusion of hexane into a solution of the Zn^{II} complex of 5,15-bis(3,5-dihydroxy-1-phenyl)octaethylporphyrin (**1**) in isobutyl benzoate (IBB) gave single crystals of a 1:2 adduct containing an additional two molecules of water, $\mathbf{1}\cdot 2H_2O\cdot 2IBB$. The IR spectra showed a significant shift (≈ 36 cm^{-1}) to lower wavenumber in $\nu_{C=O}$ for IBB upon adduct formation. Similar treatment of a solution of compound **1** in tetrahydrofuran (THF) with hexane afforded a 1:4 adduct, $\mathbf{1}\cdot 4(THF)$. The formulae of these adducts were confirmed by ^{1}H NMR and microanalyses.

Host **1** formed similar adducts with various guest molecules when crystallized from a mixture of the guest and an appropriate hydrocarbon (hexane, decane, benzene, or *p*-xylene). The host:guest stoichiometry was 1:2 for such guests as alkyl benzoates (alkyl = methyl, propyl, isopropyl, and butyl), 5-nonanone, and methyl 2-naphthyl ketone, and in some cases 1:3, for example, for styrene oxide as a guest. As in the case of adduct $\mathbf{1}\cdot 2H_2O\cdot 2IBB$, most adducts thus obtained contained two molecules of water; included carbonyl guests exhibited a characteristic complexation-induced shift in $\nu_{C=O}$. Bulky guests such as *tert*-butyl benzoate, ethyl 1-adamantenecarboxylate, and 2-adamantanone tended to give an apparently 1:3 host:guest ratio. In some cases, host – guest – hydrocarbon adducts were obtained, for example, a 1:2:3 adduct crystallized from a mixture of methyl 1-naphthylacetate and benzene. Even hydrocarbon adducts resulted in the absence of potential guests. The host – guest adducts seem to have more or less similar crystal structures, judging from the similarity in the total guest/host ratios, including water molecules as guests. Unfortunately, however, many adducts thus obtained did not form single crystals, despite various attempts at recrystallization under different conditions.

The crystal structures for adducts $\mathbf{1}\cdot 2H_2O\cdot 2IBB$ and $\mathbf{1}\cdot 4THF$ as representative single crystals were determined by X-ray diffraction and are shown in Figures 1 – 4 and Figures 5 – 7, respectively, where different moieties are shown in different colors, and hydrogen bonds are represented in light blue. The crystallographic data are summarized in Table 1. Table 2 shows characteristic angles and distances (inter-ring, intercolumn, intersheet, and hydrogen-bond distances).

Adduct $\mathbf{1\cdot 2H_2O\cdot 2IBB}$: Compound **1** gives rise to an intermolecularly hydrogen-bonded (O – H $\cdots$ O – H) 2D network, where all the porphyrin rings are nearly perpendicular with respect to the molecular sheet (Figure 1a). This is because 1) the porphyrin and resorcinol rings directly bonded are roughly orthogonal, with a dihedral angle of $\varphi = 85°$, and 2) the two resorcinol rings linked by a hydrogen bond are nearly coplanar, with a tilt angle of $\phi = 11°$, as illuminated by the side view of a molecular sheet (Figure 1b). All the porphyrin rings along a column are parallel with face-to-face and center-to-center inter-ring distances of $l^{f}_{p-p} \approx 9.8$ Å and $l^{c}_{p-p} = 9.80$ Å (Figure 1a), while those in neighboring columns are not parallel, having a small tilt angle of $\theta = 7°$ (Figure 1b) and an intercolumn distance of $l_{c-c} = 18.14$ Å (Figure 1a).

Each cyclophane-like cavity is capped top and bottom by the porphyrin rings, which are doubly linked by the hydrogen-bonded chains. The two O – H $\cdots$ O – H moieties in each chain are further bridged by water, to which is hydrogen-bonded the IBB guest, as shown in Figure 2a (front view) and 2c (top view). The hydrogen bonds involved are explained in Figure 2b and their lengths (l_{o-o}) are summarized in Table 2.

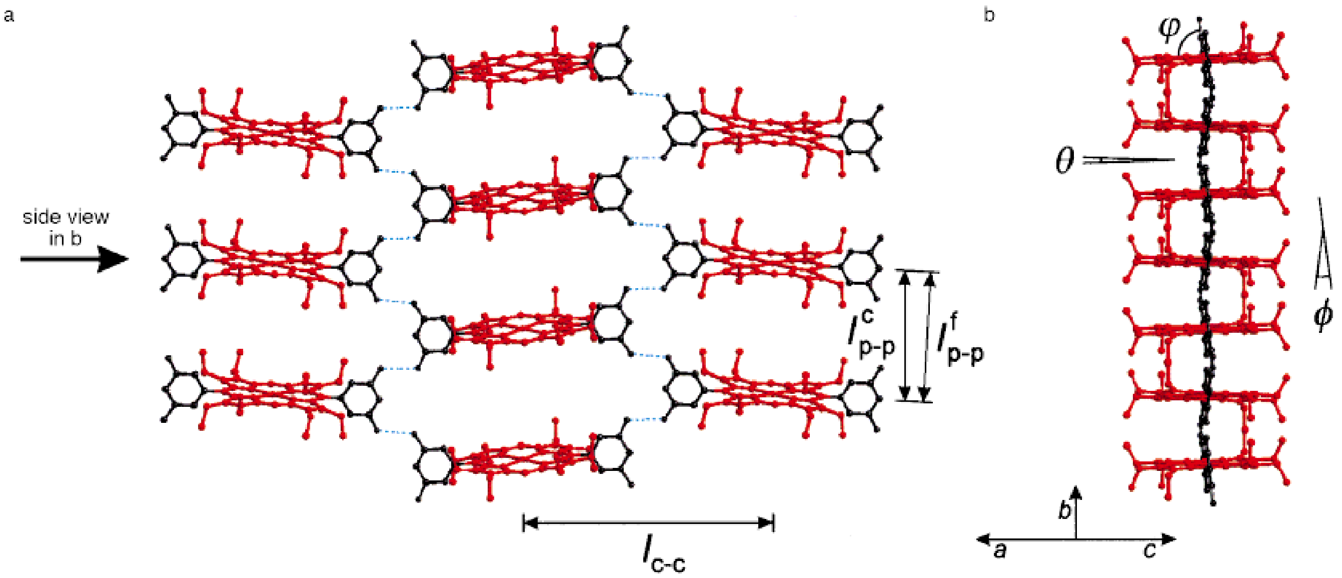

Figure 1. Structure of a molecular sheet maintained by hydrogen bonding in the crystal of adduct $\mathbf{1}\cdot 2H_2O\cdot 2IBB$: a) front view and b) side view. Porphyrin and resorcinol rings are shown in red and black, respectively, and hydrogen bonds are in light blue.

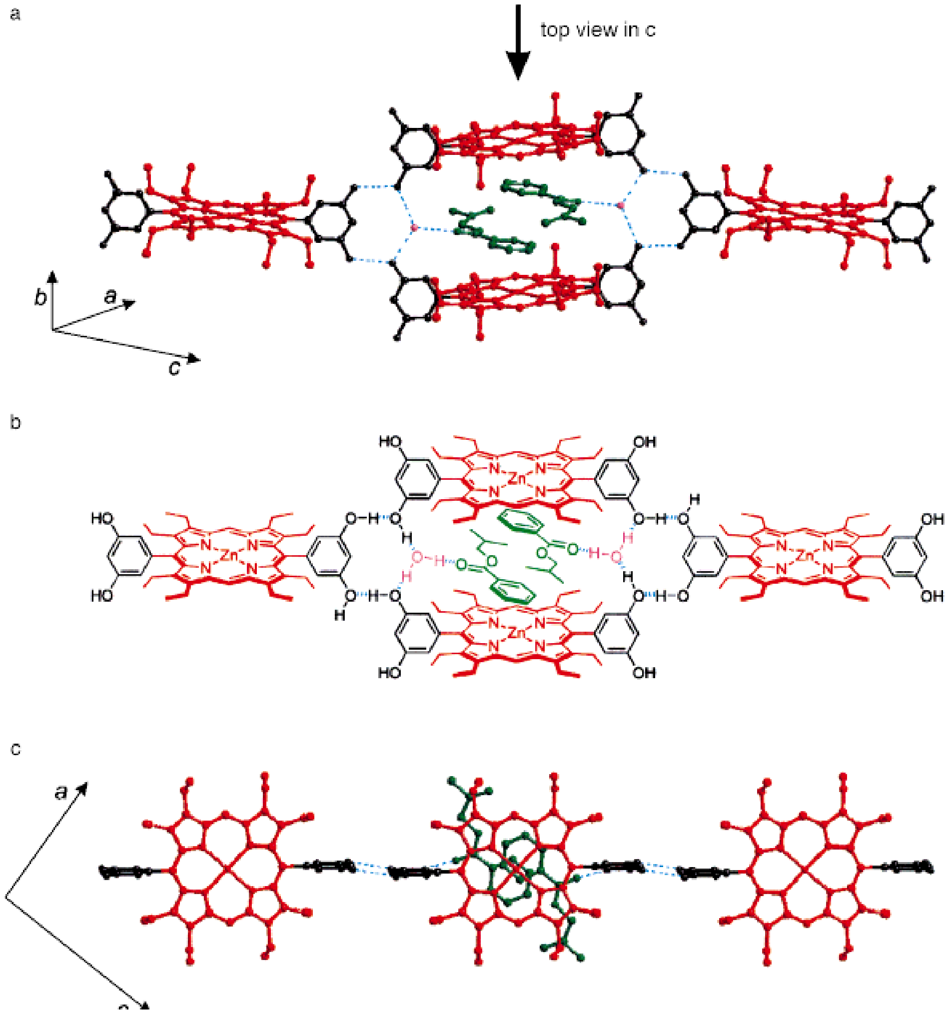

Figure 2. Structure of a guest-binding cavity in the crystal of adduct $\mathbf{1}\cdot 2H_2O\cdot 2$IBB: a) front view and b) its explanation, and c) top view. Water and IBB molecules are shown in pink and green, respectively. Other colors have the same meanings as in Figure 1.

The two IBB molecules incorporated are antiparallel with each other and nearly parallel with the porphyrin ring with an inter-ring distance of ≈ 3.3 Å.

The molecular sheets are layered with an intersheet distance of $l_{s\text{-}s} = 9.04$ Å in a staggered manner, as shown in the top view (Figure 3a) of three neighboring sheets. The intersheet space is filled with peripheral ethyl groups of the porphyrin and isobutyl groups of the guest. The porphyrin rings in different sheets share their mean planes, as shown in the side view (Figure 3b) of three adjacent columns (1, 2, and 3) in neighboring sheets. Hence, the guest-binding cavities form extended intersheet channels along the *c* axis (Figure 4).

Adduct 1·4THF: The crystal structure of the THF adduct has many aspects in common with those of the IBB adduct discussed above as far as the concomitantly generated infinite 2D networks and supramolecular cavities are concerned (Figure 5a). One of the big differences lies in the tilt angle of the two hydrogen-bonded resorcinol rings; $\phi = 55^\circ$ (Figure 5b), compared with $\phi = 11^\circ$ in adduct $\mathbf{1}\cdot 2H_2O\cdot 2$IBB. Thus, the poly(resorcinol) chains and hence the porphyrin rings attached to the chain ($\theta = 72^\circ$) are arranged in zigzags, since the porphyrin and resorcinol rings in compound **1** are again almost orthogonal ($\varphi = 89^\circ$) (Figure 5b). The consequences of these structural features are that 1) the porphyrin rings are significantly tilted with respect to the molecular sheet and hence form highly slipped columns with $l^{f}_{p\text{-}p} \approx 7.4$ Å and $l^{c}_{p\text{-}p} = 9.12$ Å, and 2) those in neighboring columns with $l_{c\text{-}c} = 17.02$ Å are far from parallel with each other (Figure 7b).

Four molecules of THF are bound in or near each cavity, two by hydrogen bonding at the resorcinol sites ($O{-}H\cdots O{-}H\cdots$THF) and two by metal coordination (Zn$^{II}\cdots$THF) (Figure 6); the Zn–O distance is 2.56 Å and the N-Zn-O angle is 87.4 or 89.4°n. The central Zn^{II} ion is thus hexacoordinated, although Zn^{II} porphyrins are usually tetra- or pentacoordinated.[12] The metal-bound THF molecules are disordered; this is why they appear as six-membered rings in Figure 6.

The zigzag nature also affects the packing modes of molecular sheets (Figure 7a). The neighboring sheets slide laterally by an intercolumn distance ($l_{c\text{-}c}$), so that porphyrin rings tilting in opposite directions are brought into proximity. This is best seen in the side view (Figure 7b) of three neighboring columns (1, 2, and 3) in neighboring sheets. Such an offset geometry of the herringbone type allows intersheet edge-to-face porphyrin-porphyrin contacts or, more precisely, van der Waals interactions between porphyrin rings and peripheral ethyl groups.

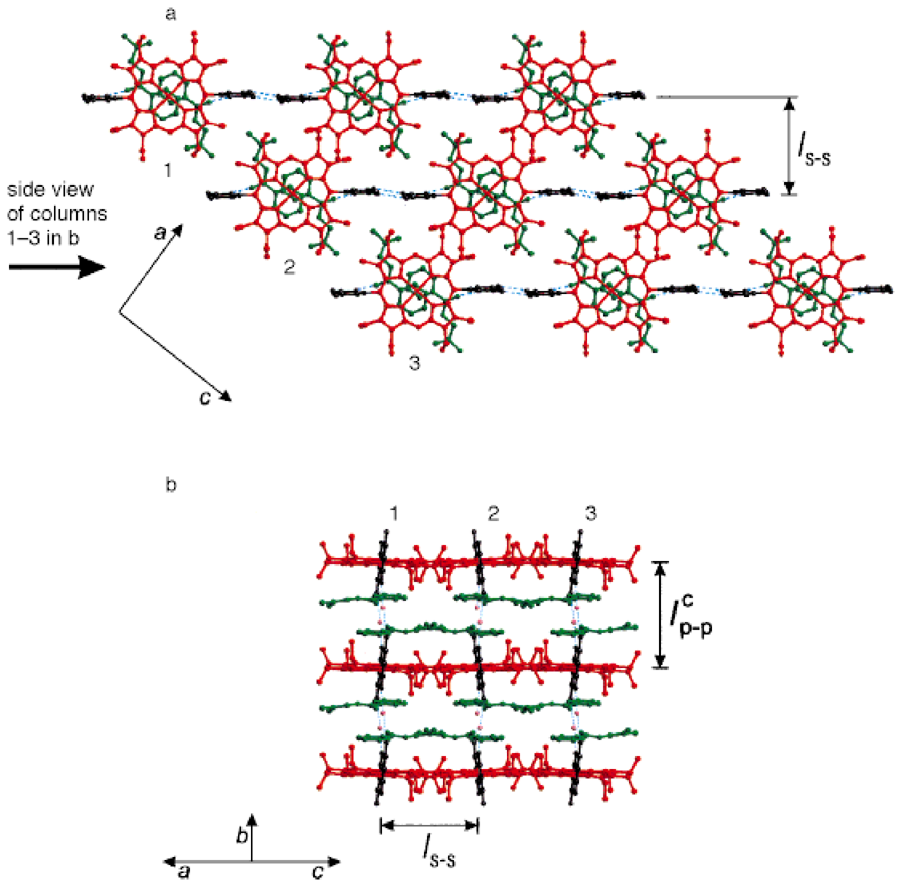

Figure 3. Arrangement of three neighboring molecular sheets in the crystal of adduct $\mathbf{1}\cdot 2H_2O\cdot 2$IBB: a) top view of the sheets and b) side view of three adjacent porphyrin columns (1, 2, and 3) in neighboring sheets. Different colors have the same meanings as in Figure 2.

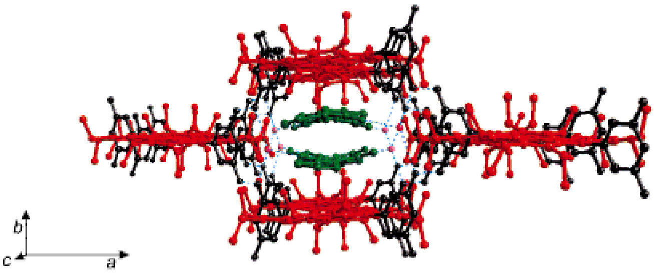

Figure 4. Perspective view along the *c* axis of the guest-binding cavities in the crystal of adduct $\mathbf{1}\cdot 2H_2O\cdot 2$IBB. Different colors have the same meanings as in Figure 2.

The observed sliding mode in $\mathbf{1}\cdot 4$THF is in contrast to a lateral slide of the sheets by half an intercolumn distance ($0.5l_{c\text{-}c}$) to give a staggered geometry for adduct $\mathbf{1}\cdot 2H_2O\cdot 2$IBB (Figure 3a). The different layer structures may be understood in terms of crystal packing. In the IBB adduct, the in-cavity space is effectively filled by the large IBB molecules, while the out-of-cavity space in the vicinity of the resorcinol moieties remains vacant (Figure 2c). In the THF adduct, this space is at least partially filled by the hydrogen-bonded THF molecules, while two molecules of metal-bound THF are too small to fill the in-cavity space (Figure 6b). In both cases, the empty space has to be filled by the peripheral alkyl groups of the porphyrin. This may

Table 1. Crystal data for adducts $\mathbf{1}\cdot 2H_2O\cdot 2$IBB and $\mathbf{1}\cdot 4$THF.

	$\mathbf{1}\cdot 2H_2O\cdot 2$IBB	$\mathbf{1}\cdot 4$THF
formula	$C_{70}H_{84}N_4O_{10}Zn$	$C_{64}H_{84}N_4O_8Zn$
M_r	1206.83	1102.77
crystal size (mm)	0.10 × 0.15 × 0.20	0.15 × 0.15 × 0.25
crystal color	reddish purple	reddish purple
crystal system	monoclinic	monoclinic
space group	$C2/c$	$P2_1/a$
a (Å)	22.329(1)	19.103(2)
b (Å)	9.7961(5)	9.116(3)
c (Å)	29.394(2)	19.248(2)
β (°)	92.055(4)	117.879(5)
V (Å^3)	6425.6(6)	2962.9(9)
Z	4	2
ρ_{calcd} (g cm^{-3})	1.247	1.236
radiation	$Mo_{K\alpha}$ ($\lambda = 0.71069$ Å) graphite-monochromated	$Mo_{K\alpha}$ ($\lambda = 0.71069$ Å) graphite-monochromated
μ (cm^{-1})	4.43	4.72
transmission	min. 0.925; max. 1.000	min. 0.975; max. 1.000
$2\theta_{max}$ (°)	52.6	55.0
scan mode	ω	$\omega - 2\theta$
T (K)	293	293
no. reflns measured	7085	7456
no. unique reflns	6903	7426
no. reflns used ($I > 3\sigma(I)$)	3184	3585
no. parameters	527	463
R,[a] R_w[b]	0.042, 0.049	0.062, 0.076
GoF	1.48	2.22
Final diff Four. map (e Å^{-3})	max. 0.35; min. −0.26	max. 0.58; min. −0.90

[a] $R = \Sigma \lvert \lvert F_o \rvert - \lvert F_c \rvert \rvert / \Sigma \lvert F_o \rvert$. [b] $R_w = [\Sigma w(\lvert F_o \rvert - \lvert F_c \rvert)^2 / \Sigma w F_o^2]^{1/2}$.

Table 2. Selected angles and distances for adducts $1 \cdot 2H_2O \cdot 2IBB$ and $1 \cdot 4THF$.[a]

	$1 \cdot 2H_2O \cdot 2IBB$	$1 \cdot 4THF$
φ (°)	85	89
θ (°)	7	72
ϕ (°)	11	55
l^{f}_{p-p} (Å)	9.8	7.4
l^{c}_{p-p} (Å)	9.80	9.12
l_{c-c} (Å)	18.14	17.02
l_{s-s} (Å)	9.04	9.55
l_{o-o} (Å)	2.74 (res–res) 2.71 (res–OH_2) 2.83 (H_2O–OC)	2.82 (res–res) 2.66 (res-THF)

[a] Definitions are as follows: φ, dihedral angle between porphyrin and resorcinol rings; θ, tilt angle of two porphyrin rings in neighboring columns; ϕ, tilt angle of two resorcinol rings hydrogen-bonded; l_{f}^{p-p}, face-to-face inter-ring distance in a porphyrin column; l_{c}^{p-p}, center-to-center inter-ring distance in a porphyrin column; l_{c-c}, intercolumn distance of neighboring porphyrin columns; l_{s-s}, intersheet distance of neighboring molecular sheets; l_{o-o}, O–O distance in a hydrogen bond between two resorcinol moieties (res–res), resorcinol and water (res–OH_2), resorcinol and THF (res–THF), or water and IBB.

be achieved most effectively when the IBB and THF adducts adopt parallel staggered geometry (Figure 3) and tilted edge-to-face geometry (Figure 7), respectively.

The apohost and guest binding: Both adducts lose their included guest molecules when heated, as readily monitored by thermal gravimetry. The loss of four THF molecules from adduct $1 \cdot 4THF$ apparently occurs in a single step in a temperature range of 110–150 °C at a rate of temperature change of 10 °C min^{-1}. In contrast, that of two IBB molecules from adduct $1 \cdot 2H_2O \cdot 2IBB$ occurs in a stepwise manner at 90–160 °C and 160–180 °C for the first and second molecules, respectively; water molecules seem to be lost at 60–100 °C.The resulting guest-free apohost is no longer a single crystal, but readily regenerates the original adducts, although not in single crystalline form, upon exposure to the vapor of the guests. Other volatile guests can also be included in this manner.

Conclusions

This work may be summarized as follows. 1) The present porphyrin derivative **1** and the previously studied anthracene derivative **2** have similar hydrogen-bonded 2D networks. This suggests that the present approach may be generalized to other orthogonal aromatic systems. The porphyrin rings, which otherwise readily self-stack, can be *deaggregated* to give crystals of a porous nature.[18] 2) The large cavities are filled by bound guests. Both adducts investigated exhibit a total host:guest ratio of 1:4. This is in marked contrast to the 1:2 stoichiometry for the anthracene system **2**, where two guest molecules are directly hydrogen-bonded to the host.[14] In the present case, two molecules of water or THF are bound in this manner. They are obviously too small to fill the cavity and allow two additional guest molecules to be bound by hydrogen bonding to the water or by metal coordination to the central Zn^{II} ion. The failure of many adducts to give single crystals might be due to the difficulty in packing the large cavities. 3) The 2D network is actually flexible and adjustable to fit guest molecules. The most favorable crystal packing is attained by adjusting the tilt angles of the resorcinol and hence the porphyrin moieties and by controlling the packing modes of molecular sheets.

Further work is now under way to shed light on the photochemical and photophysical properties and catalytic activities in the solid state of the present type of porphyrin derivatives, whose molecular alignment and microporosity are controlled on the basis of the orthogonality strategy with various guest molecules.

Experimental Section

General: Tetrahydrofuran and dichloromethane were distilled from sodium benzophenone ketyl and calcium hydride, respectively. Analytical thin-layer chromatography (TLC) was performed on silica gel 60 F_{254} plates (Merck). Wakogel C-200 was used for column chromatography. ^1H NMR spectra were recorded on a JEOL JNM-EX400 spectrometer. IR spectra

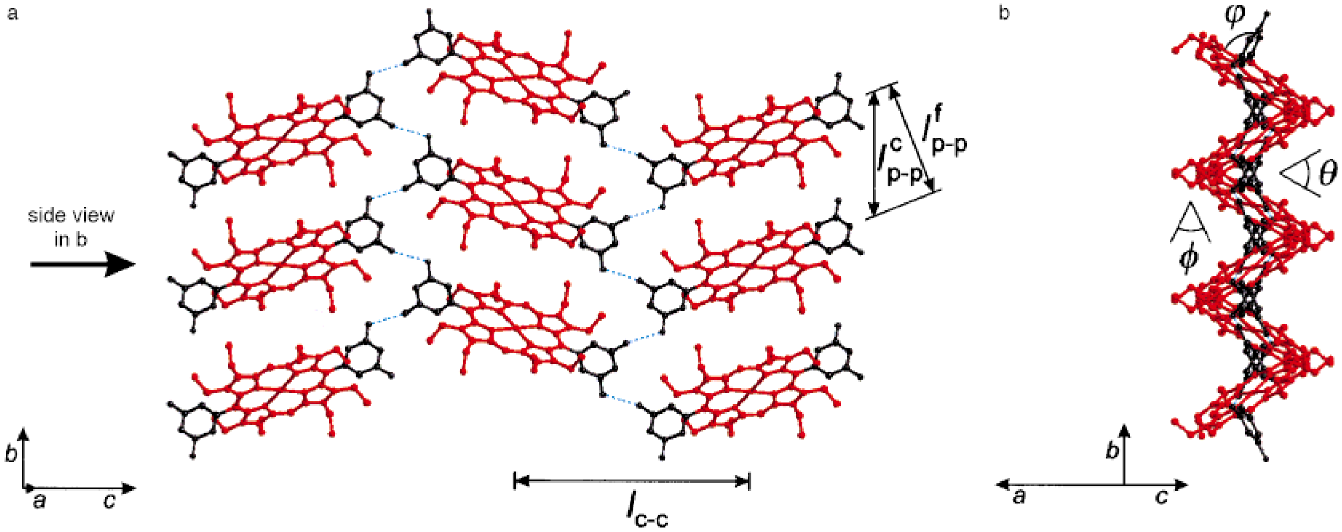

Figure 5. Structure of a molecular sheet maintained by hydrogen bonding in the crystal of adduct $1 \cdot 4THF$: a) front view and b) side view. Different colors have the same meaning as in Figure 1.

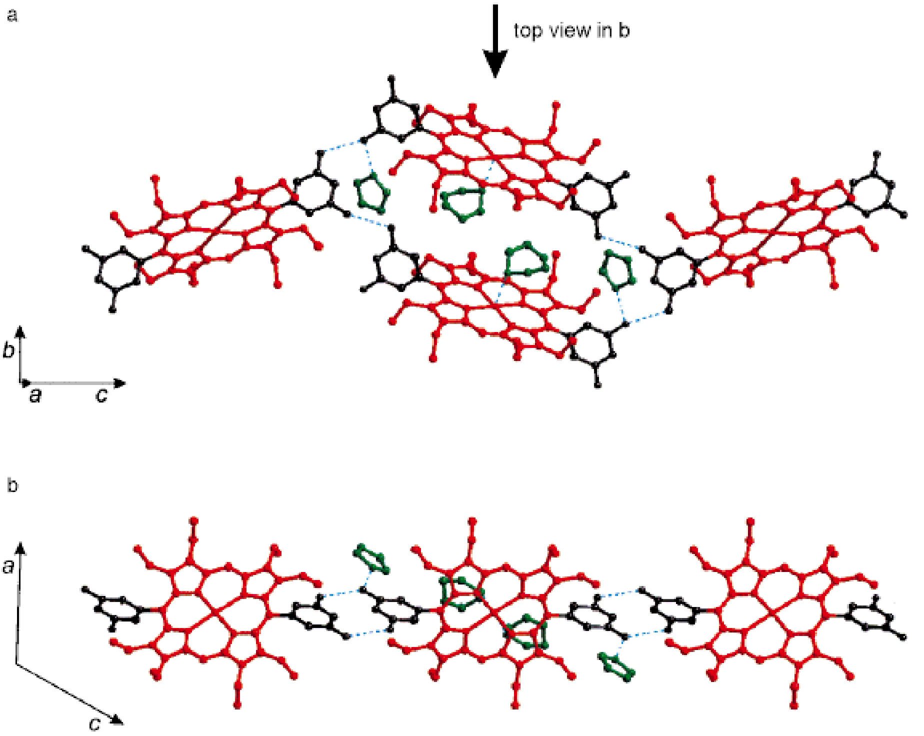

Figure 6. Structure of a guest-binding cavity in the crystal of adduct **1**·4THF: a) front view and b) top view. THF molecules are shown in green. Other colors have the same meanings as in Figure 5.

were obtained with a JASCO IR-810 spectrophotometer. Microanalyses were performed at the microanalysis center of Kyushu University.

Zinc porphyrin **1** was obtained by zinc insertion into the corresponding free base porphyrin **3**, which in turn was prepared by the acid-catalyzed condensation–cyclization of dipyrrolylmethane and dimethoxybenzaldehyde, followed by demethylation of the resulting tetramethoxy derivative **4**.

5,15-Bis(3,5-dimethoxy-1-phenyl)-2,3,7,8,12,13,17,18-octaethylporphyrin (4): Boron trifluoride etherate (53.0 mL, 0.431 mmol) was added to a solution of freshly prepared 3,3′,4,4′-tetraethyl-2,2′-dipyrrolylmethane[19] (668 mg, 2.59 mmol) and 3,5-dimethoxybenzaldehyde (430 mg, 2.59 mmol) in CH_2Cl_2 (74 mL) under nitrogen and the mixture was stirred at RT for 3 h.[20] Chloranil (954 mg, 3.88 mmol) was added and the mixture was refluxed while being stirred for 1 h, treated with triethylamine (60.0 mL, 0.431 mmol), and evaporated. The crude residue was washed with MeOH and purified by means of chromatography on silica gel (CH_2Cl_2/hexane 4:1) followed by recrystallization from CH_2Cl_2/hexane to give tetramethoxyporphyrin **4** (493 mg, 0.611 mmol, 47% yield). M.p. 259–260 °C; $R_f = 0.21$ (CH_2Cl_2/hexane 4:1); ^1H NMR (400 MHz, $CDCl_3$, 25 °C, TMS): $\delta = -2.14$ (s, 2H), 1.31 (t, $J = 7.6$ Hz, 12H), 1.88 (t, $J = 7.6$ Hz, 12H), 2.96 (q, $J = 7.6$ Hz, 8H), 3.94 (s, 12H), 4.03 (q, $J = 7.6$ Hz, 8H), 6.92 (t, $J = 2.4$ Hz, 2H), 7.39 (d, $J = 2.4$ Hz, 4H), 10.25 (s, 2H); ^{13}C NMR (100 MHz, $CDCl_3$, 25 °C, TMS): $\delta = 18.05$, 18.55, 19.83, 20.69, 55.60, 96.85, 101.16, 112.48, 117.53, 141.04, 142.43, 143.18, 144.36, 144.85, 158.92; $C_{52}H_{62}N_4O_4$ (807.1): calcd C 77.39, H 7.74, N 6.94; found C 77.17, H 7.72, N 6.93.

5,15-Bis(3,5-dihydroxy-1-phenyl)-2,3,7,8,12,13,17,18-octaethylporphyrin (3): Boron tribromide (462 mL, 4.87 mmol) was added to a solution of tetramethoxy derivative **4** (493 mg, 0.611 mmol) in CH_2Cl_2 (35 mL) at 0 °C over a period of 0.5 h.[21] The mixture was stirred for 1.5 h at 0 °C and for 18 h at RT, poured into a saturated aqueous $NaHCO_3$ solution (300 mL), and extracted with EtOAc (2 × 300 mL). The extracts were combined, washed with saturated aqueous NaCl solution (300 mL), dried (Na_2SO_4), and evaporated. The residue was chromatographed on silica gel (EtOAc/hexane 1:1–4:1). The main porphyrin fraction was recrystallized from THF/hexane to give **3**·$2H_2O$·2THF (303 mg, 0.403 mmol, 66% yield for **3**). M.p. > 400 °C; $R_f = 0.26$ (EtOAc/hexane 1:1); ^1H NMR (400 MHz, $[D_6]$DMSO, 25 °C, TMS): $\delta = -2.36$ (s, 2H), 1.34 (t, $J = 7.6$ Hz, 12H), 1.75 (m, 4H, THF), 1.85 (t, $J = 7.6$ Hz, 12H), 3.04 (q, $J = 7.6$ Hz, 8H), 3.59 (m, 4H, THF), 4.04 (q, $J = 7.6$ Hz, 8H), 6.67 (t, $J = 2.2$ Hz, 2H), 6.99 (d, $J = 2.2$ Hz, 4H), 9.60 (s, 4H), 10.24 (s, 2H); ^{13}C NMR (100 MHz, $[D_6]$DMSO, 50 °C, TMS): $\delta = 17.75$, 18.39, 19.09, 20.10, 25.11 (THF), 67.00 (THF), 96.21, 102.79, 112.75, 118.26, 140.15, 141.48, 142.55, 143.88, 144.76, 156.73; $C_{56}H_{74}N_4O_8$ (**3**·$2H_2O$·2THF) (931.2): calcd C 72.23, H 8.01, N 6.02; C 71.98, H 8.02, N 5.96.

5,15-Bis(3,5-dihydroxy-1-phenyl)-2,3,7,8,12,13,17,18-octaethylporphinatozinc(II) (1): A solution of free base porphyrin **3** (303 mg, 0.403 mmol) in MeOH (90 mL) was treated with a MeOH solution (3 mL) saturated with $[Zn(OAc)_2]\cdot 2H_2O$ under reflux for 1 h.[22] The methanol was removed in vacuo. The residue was dissolved in EtOAc (100 mL), washed with water (100 mL), and evaporated. The reddish-purple crude product was purified by column chromatography on silica gel (EtOH/hexane 1:19) followed by recrystallization from THF/hexane to give **1**·4THF (264 mg, 0.324 mmol, 80% yield for **1**) as reddish purple prisms. M.p. > 400 °C; $R_f = 0.25$ (EtOH/hexane 1:19); ^1H NMR (400 MHz, $[D_6]$DMSO, 25 °C, TMS): $\delta = 1.28$ (t, $J = 7.3$ Hz, 12H), 1.75 (m, 4H, THF), 1.82 (t, $J = 7.6$ Hz, 12H), 2.92 (q, $J = 7.3$ Hz, 8H), 3.59 (m, 4H, THF), 3.96 (q, $J = 7.6$ Hz, 8H), 6.63 (t, $J = 2.0$ Hz, 2H), 6.98 (d, $J = 2.0$ Hz, 4H), 9.46 (s, 4H), 10.00 (s, 2H); $C_{64}H_{84}N_4O_8Zn$ (**1**·4THF) (1102.8): calcd C 69.71, H 7.68, N 5.08; found C 69.82, H 7.71, N 5.07. Slow diffusion of hexane into a solution of compound **1** in isobutyl benzoate (IBB) afforded adduct **1**·$2H_2O$·2IBB; $C_{70}H_{84}N_4O_{10}Zn$ (1206.8): calcd C 69.67, H 7.02, N 4.64; found C 69.62, H 7.00, N 4.63.

X-Ray crystallography: A single crystal of an adduct was mounted in a glass capillary or on a glass fiber. Diffraction data were collected on an Enraf Nonius CAD4 (for adduct **1**·$2H_2O$·2IBB) or a Rigaku AFC7R (for adduct **1**·4THF) four-circle automated diffractometer. The unit cell parameters used for refinement were determined by least-squares calculations on the setting angles of 25 reflections in the range of $2\theta = 20-25°$ or $23-29°$. Reflection data were corrected for both Lorentz and polarization effects, but no absorption correction was applied.

The structures were solved by the direct methods with the programs SAPI90 or SIR92 and the Fourier techniques used DIRDIF94. Non-hydrogen atoms were refined anisotropically by full-matrix least-squares calculations. Some hydrogen atoms were refined isotropically and the rest were introduced at calculated positions. The weighting scheme was $w^{-1} = [\sigma^2(F_o) + 0.00040(F_o)^2]$ for adduct **1**·$2H_2O$·2IBB or $w^{-1} = [\sigma^2(F_o) + 0.00022(F_o)^2]$ for adduct **1**·4THF. Atomic scattering factors and anomalous dispersion terms were taken from *International Tables for X-Ray Crystallography*.[23] The calculations were performed on an INDY workstation with the teXsan crystallographic software package from the Molecular Structure Corporation. The crystal structures were visualized with the Cerius2 set of computer programs of Molecular Simulations Incorporated.

Crystallographic data (excluding structural factors) for the structures reported in this paper have been deposited with the Cambridge Crystallographic Data Centre as supplementary publication no. CCDC-100433. Copies of the data can be obtained free of charge on application to CCDC, 12 Union Road, Cambridge CB2 1EZ, UK (Fax: Int code + (1223)336-033; E-mail: deposit@ccdc.cam.ac.uk).

Acknowledgements: This work was supported by CREST (Core Research for Evolutional Science and Technology) of the Japan Science and Technology Corporation and also by grants-in-aid for COE research Design and Control of Advanced Molecular Assembly Systems (no. 08CE2005) from the Ministry of Education, Science, and Culture of the Japanese Government.

Received: May 20, 1997 [F697]

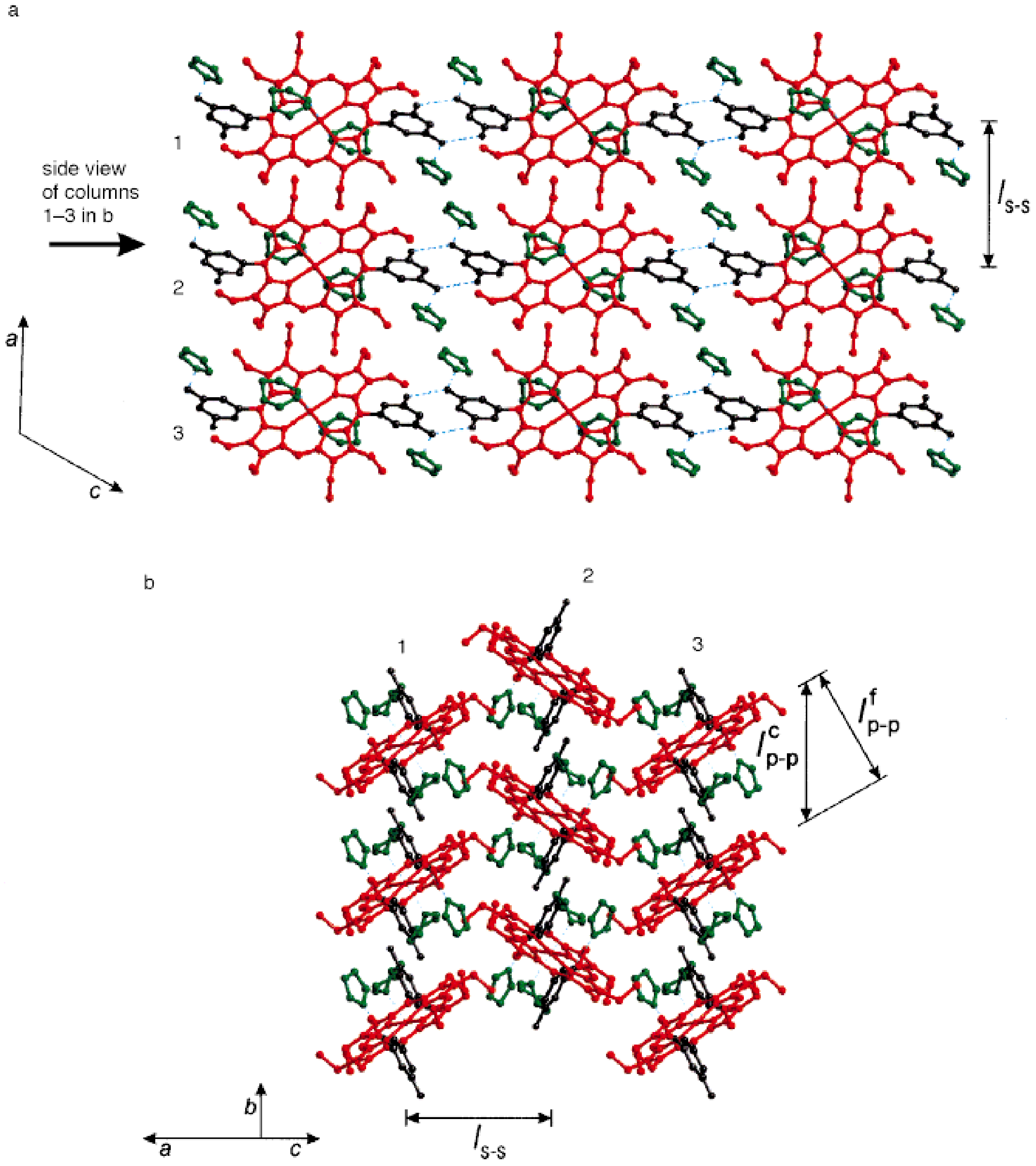

Figure 7. Arrangement of three neighboring molecular sheets in the crystal of adduct **1**·4THF: a) top view of the sheets and b) side view of three adjacent porphyrin columns (1, 2, and 3) in neighboring sheets. Different colors have the same meanings as in Figure 6.

---

[1] a) G. M. Whitesides, J. P. Mathias, C. T. Seto, *Science* **1991**, *254*, 1312–1319; b) G. M. Whitesides, E. E. Simanek, J. P. Mathias, C. T. Seto, D. N. Chin, M. Mammen, D. M. Gordon, *Acc. Chem. Res.* **1995**, *28*, 37–44; c) D. S. Lawrence, T. Jiang, M. Levett, *Chem. Rev.* **1995**, *95*, 2229–2260.

[2] a) M. R. Wasielewski, *Chem. Rev.* **1992**, *92*, 435–461; b) D. Gust, T. A. Moore, A. L. Moore, *Acc. Chem. Res.* **1993**, *26*, 198–205; c) J. Barber, B. Andersson, *Nature* **1994**, *370*, 31–34.

[3] a) P. G. Schouten, J. M. Warman, M. P. de Haas, M. A. Fox, H. L. Pan, *Nature* **1991**, *353*, 736–737; b) M. P. O'Neil, M. P. Niemczyk, W. A. Svec, D. Gosztola, G. L. Gaines III, M. R. Wasielewski, *Science*, **1992**, *257*, 63–65; c) S. Prathapan, T. Johnson, J. S. Lindsey, *J. Am. Chem. Soc.* **1993**, *115*, 7519–7520; d) R. Wagner, J. S. Lindsey, *ibid.* **1994**, *116*, 9759–9760; e) R. Wagner, J. S. Lindsey, J. Seth, V. Palaniappan, D. F. Bocian, *ibid.* **1996**, *118*, 3996–3997.

[4] For the structure of the reaction center, see: a) J. Deisenhofer, O. Epp, K. Miki, R. Huber, H. Michel, *J. Mol. Biol.* **1984**, *180*, 385–398; b) J. Deisenhofer, H. Michel, *Angew. Chem. Int. Ed. Engl.* **1989**, *28*, 829–847; c) M. G. Cory, M. C. Zerner, *J. Am. Chem. Soc.* **1996**, *118*, 4148–4151.

[5] For the structure of the light-harvesting complexes, see: a) W. Kühlbrandt, D. N. Wang, Y. Fujiyoshi, *Nature* **1994**, *367*, 614–621; b) G. McDermott, S. M. Prince, A. A. Freer, A. M. Hawthornthwaite-Lawless, M. Z. Papiz, R. J. Cogdell, N. W. Isaacs, *ibid.* **1995**, *374*, 517–521.

[6] a) A. Helms, D. Heiler, G. McLendon, *J. Am. Chem. Soc.* **1992**, *114*, 6227–6238; b) H. L. Anderson, *Inorg. Chem.* **1994**, *33*, 972–981; c) A. Osuka, S. Marumo, N. Mataga, S. Taniguchi, T. Okada, I. Yamazaki, Y. Nishimura, T. Ohno, K. Nozaki, *J. Am. Chem. Soc.* **1996**, *118*, 155–168; d) D. L. Officer, A. K. Burrell, D. C. W. Reid, *Chem. Commun.* **1996**, 1657–1658.

[7] For multiporphyrin systems via hydrogen bonding, see: a) A. Harriman, D. J. Magda, J. L. Sessler, *J. Chem. Soc. Chem. Commun.* **1991**, 345–348; b) C. M. Drain, R. Fischer, E. G. Nolen, J.-M. Lehn, *ibid.* **1993**, 243–245; c) J. L. Sessler, B. Wang, A. Harriman, *J. Am. Chem. Soc.* **1995**, *117*, 704–714; d) Y. Kuroda, A. Kawashima, T. Urai, H. Ogoshi, *Tetrahedron Lett.* **1995**, *36*, 8449–8452; e) P. J. F. de Rege, S. A. Williams, M. J. Therien, *Science* **1995**, *269*, 1409–1413; f) C. M. Drain, K. C. Russell, J.-M. Lehn, *Chem. Commun.* **1996**, 337–338. For multiporphyrin systems via metal-coordination, see: g) Y. Kobuke, H.

Miyaji, *J. Am. Chem. Soc.* **1994**, *116*, 4111–4112; h) A. Harriman, F. Odobel, J.-P. Sauvage, *ibid.* **1995**, *117*, 9461–9472; i) M. J. Crossley, P. L. Burn, S. J. Langford, J. K. Prashar, *J. Chem. Soc. Chem. Commun.* **1995**, 1921–1923; j) D. B. Amabilino, C. O. Dietrich-Buchecker, J.-P. Sauvage, *J. Am. Chem. Soc.* **1996**, *118*, 3285–3286; l) R. Stibrany, J. Vasudevan, S. Knapp, J. A. Potenza, T. Emge, H. J. Schugar, *ibid.* **1996**, *118*, 3980–3981.

[8] a) G. R. Desiraju, *Crystal Engineering: The Design of Organic Solids*, Elsevier, New York, **1989;** b) M. C. Etter, *Acc. Chem. Res.* **1990**, *23*, 120–126; c) J. C. MacDonald, G. M. Whitesides, *Chem. Rev.* **1994**, *94*, 2383–2420; d) J. Bernstein, R. E. Davis, L. Shimoni, N. L. Chang, *Angew. Chem.* **1995**, *107*, 1687–1706; *Angew. Chem. Int. Ed. Engl.* **1995**, *34*, 1555–1573; e) G. R. Desiraju, *ibid.* **1995**, *34*, 2311–2327.

[9] C. A. Hunter, J. K. M. Sanders, *J. Am. Chem. Soc.* **1990**, *112*, 5525–5534.

[10] For the arrangement in films and liquid crystals, see: C. Endisch, C. Böttcher, J.-H. Fuhrhop, *J. Am. Chem. Soc.* **1995**, *117*, 8273–8274; for the aggregation of bacteriochlorophyll derivatives in solution, see: H. Tamiaki, T. Miyatake, R. Tanikaga, A. R. Holzwarth, K. Schaffner, *Angew. Chem.* **1996**, *108*, 810–812; *Angew. Chem. Int. Ed. Engl.* **1996**, *35*, 772–774.

[11] a) M. P. Byrn, C. J. Curtis, I. Goldberg, Y. Hsiou, S. I. Khan, P. A. Sawin, S. K. Tendick, C. E. Strouse, *J. Am. Chem. Soc.* **1991**, *113*, 6549–6557; b) M. P. Byrn, C. J. Curtis, Y. Hsiou, S. I. Khan, P. A. Sawin, S. K. Tendick, A. Terzis, C. E. Strouse, *ibid.* **1993**, *115*, 9480–9497.

[12] I. Goldberg, H. Krupitsky, Z. Stein, Y. Hsiou, C. E. Strouse, *Supramol. Chem.* **1995**, *4*, 203–221.

[13] a) B. F. Abrahams, B. F. Hoskins, R. Robson, *J. Am. Chem. Soc.* **1991**, *113*, 3606–3607; b) B. F. Abrahams, B. F. Hoskins, D. M. Michall, R. Robson, *Nature* **1994**, *369*, 727–729.

[14] a) K. Kobayashi, K. Endo, Y. Aoyama, H. Masuda, *Tetrahedron Lett.* **1993**, *34*, 7929–7932; b) Y. Aoyama, K. Endo, K. Kobayashi, H. Masuda, *Supramol. Chem.* **1995**, *4*, 229–241; c) K. Endo, T. Sawaki, M. Koyanagi, K. Kobayashi, H. Masuda, Y. Aoyama, *J. Am. Chem. Soc.* **1995**, *117*, 8341–8352; d) Y. Aoyama, K. Endo, T. Anzai, Y. Yamaguchi, T. Sawaki, K. Kobayashi, N. Kanehisa, H. Hashimoto, Y. Kai, H. Masuda, *ibid.* **1996**, *118*, 5562–5571.

[15] K. Endo, T. Koike, T. Sawaki, O. Hayashida, H. Masuda, Y. Aoyama, *J. Am. Chem. Soc.* **1997**, *119*, 4117–4122.

[16] K. Endo, T. Ezuhara, M. Koyanagi, H. Masuda, Y. Aoyama, *J. Am. Chem. Soc.* **1997**, *119*, 499–505.

[17] Also see: F. D. Lewis, J. S. Yang, C. L. Stern, *J. Am. Chem. Soc.* **1996**, *118*, 2772–2773.

[18] a) D. Venkataraman, S. Lee, J. Zhang, J. S. Moore, *Nature* **1994**, *371*, 591–593; b) O. M. Yaghi, G. Li, H. Li, *ibid.* **1995**, *378*, 703–706; c) D. Venkataraman, G. B. Gardner, S. Lee, J. S. Moore, *J. Am. Chem. Soc.* **1995**, *117*, 11600–11601.

[19] a) R. Young, C. K. Chang, *J. Am. Chem. Soc.* **1985**, *107*, 898–909; b) H. Ogoshi, K. Saita, K. Sakurai, T. Watanabe, H. Toi, Y. Aoyama, Y. Okamoto, *Tetrahedron Lett.* **1986**, *27*, 6365–6368.

[20] cf. a) J. S. Lindsey, I. C. Schreiman, H. C. Hsu, P. C. Kearney, A. M. Marguerettaz, *J. Org. Chem.* **1987**, *52*, 827–836; b) J. S. Lindsey, S. Prathapan, T. E. Johnson, R. W. Wagner, *Tetrahedron* **1994**, *50*, 8941–8968.

[21] cf. J. F. W. McOmie, D. E. West in *Organic Syntheses*, *Coll. Vol. V*, Wiley, New York, **1973**, pp. 412–414.

[22] cf. K. M. Smith, *Porphyrins and Metalloporphyrins*, Elsevier, New York, **1975**, p. 798.

[23] *International Tables for X-Ray Crystallography, Vol. 4* (Eds.: J. A. Ibers, W. C. Hamilton), Kynoch, Birmingham (UK), **1974**.